NASA TECHNICAL MEMORANDUM

NASA TM X-52919

EXPERIMENTAL STUDY OF SPECTRAL INDEX, MODE COUPLING, AND ENERGY CASCADING IN A TURBULENT, HOT-ION PLASMA

by J. Reece Roth
Lewis Research Center
Cleveland, Ohio

TECHNICAL PAPER proposed for presentation at
Twelfth Annual Meeting of the Plasma Physics
Division of the American Physical Society
Washington, D.C., November 4-7, 1970

E-6027

EXPERIMENTAL STUDY OF SPECTRAL INDEX, MODE COUPLING, AND ENERGY CASCADING IN A TURBULENT, HOT-ION PLASMA

J. Reece Roth

National Aeronautics and Space Administration
Lewis Research Center
Cleveland, Ohio

ABSTRACT

The spectrum of electrostatic potential fluctuations was measured with a capacitive probe in a steady-state, turbulent plasma confined in a magnetic mirror geometry. The plasma conditions ranged over $5\times10^7 \leq n_e \leq 5\times10^8/cm^3$, $8 \leq T_e \leq 38$ eV, $350 \leq T_i \leq 930$ eV, and $B_{max} = 1.0T$. When oscillation peaks were absent, the background spectrum of electrostatic potential fluctuations had a power-law dependence on frequency of the form $\phi = \phi_o \nu^{-n}$ over the range 0.2 to 1.0 MHz. The value of the spectral index n depended on the probe position in the magnetic field, and, at a given position, depended on the plasma characteristics. The spectral index was generally below the value $n = 2.5$ predicted by some turbulence theories formulated in k-space. Enhancement of the turbulent spectrum on the high frequency side of oscillation peaks indicates that the direction of net energy flow in the turbulent spectrum is from low frequencies to high frequencies in this plasma. The effects of a sinusoidal external modulation of the anode voltage were assessed over the range 0-100 kHz. The spectra exhibited several mode coupling phenomena, including enhanced harmonics of the externally imposed frequency, and sideband modulation of internally generated oscillation peaks. External excitation of the plasma at frequencies below 50 kHz resulted in only a small degree of ion heating.

INTRODUCTION

The determination of the spectrum of plasma turbulence is a central problem of non-linear plasma theory. A number of theories of plasma turbulence have been formulated[1-7]. These theories contain significant differences of detail, but all predict a power law spectrum of electrostatic potential fluctuations, ϕ, of the form

$$\phi = \phi_o k^{-m} \qquad (1)$$

Under the conditions approximating the present experiment, for large values of the wave number k, several of these theories [1,3,4,5,7] further predict a spectral index of $m = 5$ for potential fluctuations at large values of k, identified with the regime of collisionless dissipation by Tchen[7]. Other theories[2,5] predict smaller values of the spectral index for neutral-dominated[2] or collision-dominated[5] plasmas.

These analyses are based on one or more simplifying assumptions, including that of an infinite, unbounded plasma, and it would not be surprising to find that a simple power law expression with $m = 5$ does not hold in general. As has been pointed out by Tchen[7], Eq. (1) with $m = 5$ cannot be fully valid, since one would expect the magnitude of the spectrum to depend on the rate of dissipation, which is itself dependent on wavenumber. In addition to this difficulty, these theories do not take into account the effects of gradients of the plasma properties or of the magnetic field. It is therefore of some theoretical interest to discover whether, in a laboratory plasma, the spectral index in Eq. (1) depends upon the presence or absence of gradients of these quantities, or upon the magnitude of the plasma properties.

Attempts have been made to determine the nature of plasma turbulence by using a Langmuir probe to measure such fluctuating plasma parameters as ion saturation current[1,8-13] or floating potential[8,10,12,14-16]. The spectrum of fluctuations in uhf emission from a plasma, near 1.0 GHz, was studied by Apel[17].

These experimental approaches to the problem of plasma turbulence have required the assumption that the frequency, ω, and wavenumber, k, of the fluctuations are related by a constant factor

$$\omega \approx k \qquad (2)$$

since the theories are expressed in k-space, but the experimental equipment required to perform the measurements renders it expedient to measure the fluctuations in ω-space.

In addition to this fundamental assumption, two additional assumptions are implicit in the use of Langmuir probes for such measurements. One assumption is that the frequency response of the Langmuir probe is unaffected by the plasma-probe sheath, and the second is that this interaction does not generate spurious noise that might mask the plasma turbulence. There is evidence that both assumptions may be violated. Serafini[12] has shown that the frequency spectrum of a Langmuir probe operating at ion saturation differs substantially from the spectrum of electrostatic potential fluctuations detected by a capacitive probe at frequencies above 1.0 MHz. These results suggest the possibility that the Langmuir probe frequency response may fall off at frequencies above 1.0 MHz, and hence give an incorrect potential spectrum. This fall-off in the frequency response of Langmuir probes (relative to that of capacitive probes) was observed in other investigations[18].

In addition to this difficulty with the frequency response of Langmuir probes, there have been suggestions in the recent literature that the interaction of a Langmuir probe with a plasma may generate spurious fluctuations not present in the undisturbed plasma[19,20]. The presence of "spurious" noise from 7 to 10 MHz on the signal from a floating Langmuir probe, not observed with a capacitive probe, was measured in paired comparison studies of these two types of probes[18]. Over the frequency range of the present investigation, $0.2 \leq \nu < 1.0$ MHz, essentially identical results were obtained for data taken with Langmuir and capacitive probes, although only the latter are reported herein.

In the present investigation, spectra of electrostatic potential fluctuations were taken with a capacitive probe over the range 0.2 to 1.0 MHz. The effects of changes in plasma conditions on the turbulent spectrum and upon spectral index were investigated. These results appear to be in conflict with existing theories of plasma turbulence. Data were taken which appear relevant to the determination of the sense of net energy cascading along the turbulent spectrum in frequency space. A subsequent series of experimental runs were taken to investigate the nature of the mode coupling and ion heating by an externally imposed excitation of the turbulent spectrum.

EXPERIMENTAL ARRANGEMENTS

A photograph of the modified Penning discharge used in this experiment is shown in Fig. 1. The plasma is confined in a superconducting magnetic mirror apparatus[22] with a mirror ratio of 2.6:1. The maximum field on the axis occurs at the magnetic mirrors, and can be varied up to 2.0 Tesla. Unless noted otherwise, the maximum magnetic field was set at 1.0 T in the present investigation. The plasma is 15 cm in diameter at the midplane, and can be operated in the steady state for durations up to several hours[23].

When a high DC potential is applied to the anode ring (the vertical element at the center of Fig. 1), thermalized ions of high kinetic temperature are observed coming out through the mirrors[23,24]. On Fig. 2 is shown a retarding potential curve for such ions.[23] These ions have a quite accurately Maxwellian energy distribution along a radius in velocity space, even in the high-energy tail. The electron energy was typically more than a factor of 10 below in the ion kinetic temperature in this plasma. The dependence of the ion kinetic temperature on the discharge operating conditions is shown in Fig. 3. This figure shows the ion kinetic temperature plotted as a function of the DC anode voltage, for four different background pressures of deuterium gas. An objective of the present investigation was to identify the nature of the processes responsible for this thermalization and heating of the ions.

Deuterium gas was used in the present investigation. The range of operating conditions of this plasma is shown in Table I. The mean free paths of all binary charged-neutral collisions were much greater than the apparatus dimensions, and the energy density of the plasma was no less than that of the background neutral gas. The electrostatic potential spectra should therefore be characteristic of the plasma, and not of fluctuations in the background neutral gas. The measurements of spectral index were made under plasma operating conditions such that no oscillation peaks or their harmonics interfered with the smooth background spectrum in the frequency range covered.

The principal equipment used in this investigation is shown in Fig. 4. During the mode-coupling measurements described below the high voltage DC power supply was connected to the anode ring through an inductor, to isolate this supply from the AC power applied to the anode ring. During these mode-coupling investigations, a powerful AC amplifier was also connected to the anode ring though a suitable capacitor, to couple the AC signal to the anode ring, while at the same time isolating the AC power supply from the high voltage DC bias on the anode ring. The amplifier is capable of operating over the range 1-100 kHz, and has an output of 5 kV RMS at 5 kW. The amplifier was driven by a variable frequency oscillator, which provided a sinusoidal input signal of the desired frequency. The retarding potential energy analyzer was located in approximately the position shown in Fig. 4. The amplifier, capacitor, and inductor were removed from the circuit during the spectral index and energy cascading measurements described below.

Two capacitive probes were used to measure the electrostatic potential fluctuations in the plasma. These probes are similar to that described by Schmidt.[20] A cross-section of the probe used is shown in Fig. 5(a). The frequency response of this probe and its associated cathode follower and amplifier is shown in Fig. 5(b). The frequency response of the measuring system is essentially constant from 1 kHz to 10 MHz. Note that the ordinate of the calibration curve is the signal ratio, and is not expressed in db.

By moving the probe assembly along the magnetic field axis, the two capacitive probes could be positioned at the six locations shown in Fig. 6. These positions were chosen to help distinguish the effects on the spectral index of various combinations of radial and axial gradients of magnetic field and plasma energy density. The kinetic temperature and relative number density of the ions escaping through the magnetic mirrors were measured with a retarding potential energy analyzer.[23] Absolute values of the electron number density and kinetic temperature were measured by taking conventional Langmuir probe traces at position #5, shown in Fig. 6.

It was recognized that the experimental equipment could introduce nonlinearities into the data, and precautions were taken to avoid this. The elements of the probe system were run at all times below saturation, so that no harmonic content was introduced by signal clipping. The signal was also kept above the amplitude threshold for linear response of the equipment. During the measurements of spectral index, the high-pass filter was set to cut off all frequencies below 150 kHz, in order to avoid saturation of the spectrum analyzer and x-y recorder by large amplitude peaks, and by the continuum spectra below the frequency range of interest. In the mode coupling experiments, it was verified for the data presented here that the harmonic content of the signal appearing on the anode ring was very much smaller than the harmonics generated by the plasma itself. Two balanced probes operating in the differential mode were used to verify that none of the signal in the smooth background spectrum was a common mode, such as might arise from noise in the anode ring sheath, for example.

MEASUREMENT OF SPECTRAL INDEX

Electrostatic potential fluctuation spectra were taken from both probes at a given axial station. The probe assembly was then moved to a different axial position, with the anode voltage, tank pressure, and the other controllable parameters held fixed. Typical raw spectra are shown in Fig. 7(a) for the frequency range 0.2 to 1.0 MHz. These spectra were tabulated, corrected for small nonlinearities in the probe instrumentation, and converted to a logarithmic base. An example of the corrected data for the same two runs is plotted on a log-log scale in Fig. 7(b). The spectral indices were determined by excluding oscillation peaks, harmonics of these peaks, or data at or to the left of the knee of the curves, and then obtaining a best-fitting straight line to the remaining data with a logarithmic least-squares computer program. All spectra had a knee, due either to the high-pass filter or to the nature of the spectrum. The spectra analyzed covered no less than a factor of two in frequency, and more typically covered a factor of four in frequency.

All of the spectra taken in this investigation exhibited the power law dependence of electrostatic-potential amplitude, ϕ, on frequency, ν, given by the expression

$$\phi = \phi_o \nu^{-n} \tag{3}$$

when plasma-generated oscillation peaks were absent. The best-fitting spectral index for each set of plasma conditions and at each position in the plasma is shown in the form of a scatter plot in Fig. 8. The scatter of spectral index at a given plasma position is at least a factor of five greater than the uncertainty of an individual determination of the spectral index. It should be noted that the spectral indices shown in Fig. 8 refer to the amplitude of the electrostatic fluctuations, and should be multiplied by a factor of two to obtain the power spectral index.

An attempt was made to correlate the spectral indices at a given plasma position with the plasma density, the neutral gas density, the ion kinetic temperature, the plasma energy density, the plasma floating potential, and the amplitude ϕ_o of the turbulence. None of these produced an identifiable systematic trend in the spectral index. The only observed trend was the tendency of the median value of the spectral indices of the data obtained to be different for the six positions in the plasma, as illustrated in Fig. 8. These differences are thought to be due to the differing magnetic field conditions rather than to the different plasma densities within the magnetic bottle, since no systematic dependence of spectral index on plasma density was apparent at a given position in the magnetic field. For a given set of plasma operating conditions, different values of the spectral index were obtained at each of the six positions in the plasma. The position on the axis at the magnetic field midplane had gradients of neither magnetic field or plasma energy density, and might therefore be an approximation to an infinite plasma. The other five positions afford various combinations of energy density and magnetic field gradients.

OBSERVATION OF ENERGY CASCADING IN FREQUENCY-SPACE

The correct direction of the net energy cascade in a turbulent spectrum has been a vexing question in plasma theory for many years. Some investigators[6] have maintained that plasma turbulence is analogous to conventional hydrodynamic turbulence, in that the net turbulent energy transfer proceeds from low wavenumbers to high wave-numbers (and hence presumably to high frequencies), where it is eventually dissipated as thermal motions of the plasma constituents. Another school of thought holds that at high wavenumbers, but below the wavenumber corresponding to the Debye length, the direction of the net energy cascade is from large wavenumbers to small wavenumbers.[25]

Two sets of experimental observations were made in the course of this experiment which may have some bearing on determining the direction of the turbulent energy cascade. It should be noted that all measurements herein were made below the ion gyro frequency and the ion plasma frequency. The first class of observations is illustrated by the data discussed in the following two sections, in which subharmonics of the externally imposed oscillation peaks are not observed. The data presented in Figs. (12) and (13) below are typical in this respect of all data taken to date. One can argue that if the energy were cascading downward in frequency, then perhaps one might expect to observe subharmonics of the fundamental frequencies. The observation only of harmonics can perhaps be interpreted to imply that the turbulent energy is cascading upward in frequency.

The second set of experimental observations relevant to the direction of energy cascading are based on the following argument: If there existed a broad peak on the turbulent spectrum that coupled energy from an external source to the turbulent spectrum, then one might expect to observe one of the two situations illustrated schematically in Fig. 9. In Fig. 9(a), the energy is assumed to be cascading upward in frequency, so that an energy input at some frequency would enhance the spectral amplitude at frequencies above the frequency in question. The expected shape of the spectrum is shown as the solid line for a linear and a logarithmic plot of turbulent amplitude as a function of frequency, and it is assumed that the turbulent spectrum obeys the power-law relation given by Eq. (3).

In Fig. 9(b) is shown the situation expected if the energy is fed in at a given frequency, but cascades downward toward lower frequencies. In this case one might expect the spectrum illustrated by the solid lines, in which the additional energy input is carried to lower frequencies. By looking for one or the other of the types of spectra shown in Fig. 9, one might get an indication of the direction of energy flow in the turbulent spectrum.

A requirement for the observation of one or the other of the spectra shown in Fig. (9) is an oscillation at which energy is being injected into the turbulent spectrum. The high ion temperature of this plasma, and the Maxwellinanization of the ion energy, illustrated in Figs. 2 and 3, are indicative of significant energy transfer to the plasma. Multiple-sweep waveforms of the electrostatic potential measured with a capacitive probe are shown on Fig. (10) for five sweep rates. The low frequency oscillation at about 18 kHz prominent in Figs. 10(a) and 10(b), appears to trigger the higher frequency oscillations, and is the continuity-equation oscillation described elsewhere.[26,27] The internally generated damped oscillation at 170 kHz, prominent in Figs. 10(b) and 10(c), would appear to be the frequency at which significant energy is transferred to the ions, perhaps by the damping shown. The oscillations, observable in Figs. 10(d) and 10(e), are at the ion plasma frequency in the anode ring sheath.

On Fig. 11 are shown two examples in which the plasma operating conditions were such that the damped oscillation was at slightly higher frequencies. The upper part of the figure shows the raw spectrum between 0 and 1 MHz, and the waveform of the oscillations. The damped nature of the oscillation producing the peak is again evident. At the bottom of Fig. 11 these two examples are plotted on log-log scales. The enhancement of the spectrum <u>above</u> the oscillation peaks is quite evident. This enhancement was observed at frequencies above the oscillation peaks in all cases studied, and resembles the situation in Fig. 9(a), which would be expected for energy cascading to higher frequencies. It would appear plausible that the spectral enhancement represents an energy input to the plasma that is responsible for the observed ion heating, in whole or in part.

RESPONSE OF PLASMA TO SINUSOIDAL EXTERNAL EXCITATION

Spectra of the electrostatic potential fluctuations were taken with the circuit shown on Fig. 4, and with the AC amplifier, capacitor, and inductor in the circuit. Fig. 12(a) was taken without external excitation of the plasma, as a standard of comparison. A prominent peak is apparent at the continuity-equation oscillation frequency.[26,27] There are no subharmonic peaks visible at 1/2, 1/3, etc. of the continuity equation frequency. Clearly defined subharmonics were never observed in this experiment, although harmonics were quite common (they are off scale in Fig. 12). Occasionally a minor oscillation peak, like that shown in Fig. 12(a), would shift frequency slightly to "lock on" to a subharmonic of the excitation frequency, as illustrated in Figs. 12(e) and 12(f). In Fig. 12(a), there is no significant asymmetric enhancement on either side of the oscillation peak, presumably implying that the oscillation in question was only weakly coupled to the turbulent spectrum, if at all.

On Fig. 12(b) - 12(i) are shown spectra for the same plasma conditions that produced Fig. 12(a), but with an additional 1.5 kV rms sinusoidal signal imposed on the anode ring at the excitation frequency indicated. One can see at least two harmonics of the imposed frequency, and side bands of the continuity-equation frequency at the imposed frequency and at harmonics of the imposed frequency. The amplitude of the continuity-equation oscillation is reduced as the frequency of the external modulation approaches that of the continuity-equation oscillation. In Fig. 12(i), the continuity-equation peak is finally suppressed with the excitation frequency at 32.5 kHz.

On Fig. 13 is illustrated the phenomenon of plasma "lability", by which is meant the tendency of a plasma to generate harmonics or show improved mode coupling at certain preferred frequencies. The spectrum with no external excitation is shown in Fig. 13(a). This spectrum exhibits the continuity equation oscillation at 22.5 kHz, and three of its harmonics. The effect of a 750 V rms sinusoidal excitation is shown in Figs. 13(b) to 13(f). One effect of the external excitation is to greatly reduce the spectral amplitude of the continuity-equation oscillation. This suppression becomes more apparent as the external frequency approaches the continuity-equation frequency, until the later is scarcely apparent at an external excitation of 20 kHz. The tendency of the plasma to enhance harmonics of the imposed frequency near the continuity-equation frequency and its harmonics is quite apparent. The harmonic and sideband generation observed in the present experiment is consistent with the nonlinear effects observed by other investigators, of which the difference frequency generation reported by Krivoruchko and Kornilov[28] (1970) is an example.

EFFECT OF EXTERNAL EXCITATION ON ION KINETIC TEMPERATURE

At the outset of the present experiment, it was considered possible that the imposed AC power might be well coupled to the turbulent spectrum at the continuity-equation frequency. The effects of the external AC modulation were assessed by imposing a 5 kV RMS AC signal on the anode ring, and measuring the ion energy with the retarding potential energy analyzer shown in Fig. 4.

On Fig. 14 is shown a plot of the ion kinetic temperature as a function of the frequency of the imposed AC signal, for three background pressures of deuterium gas. These data were taken with a 20 kV DC bias on the anode ring. The data points at zero frequency are the ion energies with no external AC modulation of the anode voltage. There is a slight tendency of the ion kinetic temperature to rise with increasing frequency, amounting to almost a factor of two in energy on the lowest curve shown. The heating effect of the AC power was nevertheless not marked, and no preferred "resonant" frequency became apparent below 100 kHz. The absence of any significant heating effect of the AC power is consistent with the qualitative features of the (typical) spectral curves presented in Figs. 12 and 13. In all of these spectra, the imposed frequency appears as a sharp, narrow peak with no significant asymmetry of the background spectrum around its base. Had this imposed frequency been well coupled to the turbulent spectrum, one perhaps would expect the imposed frequency peak to be broad, of lower amplitude, and better faired in to the background spectrum.

DISCUSSION

The measurements of turbulent spectra made in the present investigation agree with current theories of plasma turbulence in that they conform to a power-law dependence, given by Eq. (3), of spectral amplitude on frequency. These measurements appear to disagree with current theories[1-7] which predict a universal power law of the form $k^{-2.5}$. The present results give ν^{-n}, where the range of n is generally below 2.5, and n depends on the plasma characteristics. A simple proportionality between ω and k, given by Eq. (2), therefore can not hold in this bounded laboratory plasma. It is perhaps not surprising that the dispersion relation for this plasma is more complicated than a simple proportionality. However, in order to obtain agreement between a $k^{-2.5}$ power law and the present results, the dispersion relation would itself have to be a power law of the form

$$k \sim \omega^p \qquad (4)$$

where

$$2.5\,p = n. \qquad (5)$$

Since there is no precedent in linearized, cold plasma theory for a dispersion relation similar to Eq. (4), with p assuming a continuous range of values depending on the plasma and magnetic field characteristics, it therefore appears that the present results are in disagreement with existing theories of plasma turbulence.

This disagreement has also been noted in isolated cases reported by other experimental investigators. Apel[17] has observed $n = 2.75$ at frequencies near 1.0 GHz; Bol and Ellis[13] have observed $n = 1.25$ or $n = 2.0$; Serafini[12] has observed $n = 1.3$; Batten et al.[8] have observed $0.5 \leq n \leq 1.0$ (Figs. 3 to 5 of Ref. 8); F. F. Chen has reported $n = 2.3$; Bol[9] has observed $n = 2.4$ (the present authors interpretation of Fig. 6 of Ref. 4), D'Angelo and Enriques[15] have observed $n = 2.4$ and 2.5, and Noon et al.[16] have observed $n = 1.0$. These investigations appear to agree with the present results in that the spectral amplitudes can be represented by a power-law relationship in frequency space, and the spectral amplitudes were generally somewhat below the value $n = 2.5$ predicted by existing theories.

By examining the turbulent spectrum in the vicinity of an oscillation peak whose waveform was observed to be damped, information was obtained that indicates that the energy transferred to the spectrum by this damping cascades upward in frequency. It would appear implausible that the spectrum would be enhanced above the oscillation peak if the energy were cascading to lower frequencies. Whenever significant enhancement of the turbulent spectrum near an oscillation peak was observed in this investigation, it was always on the high frequency side of an oscillation peak.

CONCLUSIONS

The present investigation appears to justify the following conclusions: 1.) In the absence of oscillation peaks, and over the frequency range 0.2 to 1.0 MHz, the spectral amplitude of electrostatic potential fluctuations in the plasma studied follows a power-law relation of the form $\phi = \phi_o \nu^{-n}$. 2.) The spectral index n is a function of the plasma characteristics and of the magnetic field characteristics. 3.) The spectral index varies over a range much larger than the uncertainty of an individual measurement, and the median value of the data obtained over this range is generally below the value $n = 2.5$ predicted by existing theories of plasma turbulence. 4.) The direction of net energy cascading in frequency space appears to be from low to high frequencies for the present experiment. 5.) The non-linear character of the plasma generates harmonics of an externally imposed excitation frequency, and also generates sidebands of pre-existing plasma oscillations. 6.) The plasma exhibited the phenomenon of "lability", in which harmonics of the external excitation frequency were preferentially enhanced in the vicinity of the continuity-equation oscillation and its harmonics. 7.) Externally imposed sinusoidal signals of frequencies below 50 kHz did not lead to significant heating of the ions in the plasma. 8.) A damped oscillation of undetermined origin was observed in the region of several hundred kHz, below both the ion cyclotron and ion plasma frequencies. This damped oscillation appears to be responsible for the ion heating observed in this plasma.

TABLE I

RANGE OF PLASMA CHARACTERISTICS AT PROBE LOCATION NUMBER 5

DEUTERIUM GAS, $B_{min}/B_{max} = 0.38$, $B_{max} = 1.0T$

$B_{probe} = 0.65$ T

PLASMA CHARACTERISTIC	LOW VALUE		HIGH VALUE
Neutral Number Density	$1.5x10^{12}/cm$		$2.5x10^{12}/cm^3$
Electron Number Density	$5x10^7/cm^3$		$5x10^8/cm^3$
Electron Kinetic Temperature	8.3 eV		38 eV
Ion Kinetic Temperature	350 eV		930 eV
Plasma Potential	+45 volts		+230 volts
Electron Plasma Frequency	64 MHz		202 MHz
Electron Gyro Frequency		18 GHz	
Ion Plasma Frequency (D^+)	1.0 MHz		3.3 MHz
Ion Gyro Frequency (D^+)		5 MHz	
Debye Distance	0.1 mm		6.5 mm

FIGURE CAPTIONS

1. Photograph of the plasma studied in the present investigation. The vertical element in the center is the anode ring, biased to positive potentials of up to 40 kilovolts. The plasma is approximately 15 centimeters in diameter at the midplane.
2. Typical retarding potential curve from the ion energy analyzer. The ordinate is the axial flux of ions whose energies exceed the value shown on the abscissa. The best-fitting integrated Maxwellian distribution is shown, whose ion kinetic temperature is 710 eV.
3. Relationship of DC anode voltage to deuterium ion kinetic temperature for four background pressures of deuterium. The maximum magnetic field was 2.0 T for this series of runs.
4. Schematic of apparatus used for the measurement and recording of turbulent spectra, and study of the effects of external modulation of the anode voltage. During the measurement of turbulence spectra, the two capacitive probes were mounted parallel on a forked support, one of which was on the magnetic field axis, and one of which was 3 cm off axis. The amplifier, inductor, and capacitor used for excitation of the anode ring were disconnected during the spectral index measurements.
5. (a) Cross-sectional drawing of the capacitive probe used. (b) Frequency response of the capacitive probe measuring system shown in figure 4, but without the high-pass filter.
6. Location of the six positions within the plasma at which turbulent spectra were taken with capacitive probes. Positions 2 and 5 were 9.4 cm from the midplane, at approximately the point of maximum magnetic field gradient.

Positions 4 to 6 were 3.0 cm from the magnetic axis. The mirror ratio was 2.6:1, with B_{max} = 1.0 T.

7. Two examples of the turbulence spectra taken in this investigation for a fixed set of plasma conditions, about at the midrange of Table I. Run KL-22 was taken at position 2 on Fig. 6, and KL-23 at position 4 on Fig. 6. a) the raw data, on a linear-linear scale. b) the data from (a), corrected for the system calibration and plotted on a log-log scale. Note the power-law dependence of the spectra.

8. Scatter plot of the spectral index n, from observed spectra of the form $\phi = \phi_o \nu^{-n}$, at the six positions shown in Figure 6. The scatter was a consequence of varying the plasma conditions over the range indicated in Table I, and was much larger than the error associated with a given run.

9. (a) Linear and logarithmic plot of expected electrostatic turbulence spectrum for case in which energy is added to plasma at a discrete frequency, and then cascades to higher frequencies and smaller scale sizes. (b) Linear and logarithmic plot of expected electrostatic turbulence spectrum for case in which energy is added at a discrete frequency, but cascades downward in frequency.

10. Multiple-sweep oscilloscope traces of the electrostatic potential fluctuations detected by a capacitive probe under operating conditions producing unusually coherent oscillations. Same arbitrary vertical scale is used for all five traces. Time increases from right to left.

11. Two examples of the enhancement of the turbulent spectrum at frequencies above an oscillation peak, taken at plasma conditions near the lower end of the range shown in Table I. a) Waveform, raw spectrum, and spectrum plotted on log-log scale of plasma conditions producing an oscillation at

380 kHz. Note damping of oscillation in waveform, suggesting that energy is being fed into turbulent spectrum. b) Waveform, raw spectrum, and spectrum plotted on log-log scales of plasma conditions producing an oscillation at 320 kHz.

12. Spectra illustrating the generation of harmonics and sidebands of an external excitation frequency. The D.C. anode voltage was held constant at 15 kV, and excitation amplitude at 1.5 kV rms. All spectra have the same arbitrary vertical scale, and the same 0 - 100 kHz horizontal scale. The plasma characteristics were at the lower limit of the range indicated in Table I. a) Spectrum with external excitation turned off. Note unidentified oscillation at 11 kHz, and continuity-equation oscillation at 62 kHz. b) -i) Spectra with 1.5 kV rms external excitation at frequency indicated. Note generation of harmonics of the excitation frequency, and generation of sidebands of the continuity-equation oscillation frequency at the excitation frequency and its harmonics. Note suppression of continuity equation oscillation as excitation frequency approaches one-half of its frequency.

13. Spectra illustrating plasma lability at harmonics of an external excitation frequency. The D.C. anode voltage was held constant at 2.0 kV. All spectra have the same arbitrary vertical scale, and tha same 0 to 100 kHz horizontal scale. The plasma characteristics were near the high end of the range indicated in Table I. a) spectrum with external excitation turned off. Note continuity-equation oscillation at 22.5 kHz and its harmonics. b) - f) spectrum with 750 Vrms external excitation at frequency indicated. Note suppression of the continuity-equation oscillation, and

enhancement of the harmonics of excitation frequency that lie near the continuity-equation oscillation frequency and its harmonics.

14. Ion kinetic temperature as a function of frequency of 5 kV RMS sinusoidal modulation signal, for three pressures of deuterium gas. Kinetic temperature with no modulation is plotted at zero frequency. The DC anode voltage was 20 kV for all runs.

REFERENCES

1. F. F. Chen, Phys. Rev. Letters 15, 381 (1965).
2. H. Guthart, Phys. Fluids 8, 999 (1965).
3. R. L. W. Chen, Phys. Fluids 9, 761 (1966).
4. T. K. Fowler, Phys. Fluids 9, 1437 (1966).
5. C. M. Tchen, NBS Report 8435 (1966).
6. C. M. Tchen, Phys. Fluids 8, 1659 (1965).
7. C. M. Tchen, IEEE Trans. on Electron Devices ED-17, 247 (1970).
8. H. W. Batten, H. L. Smith and H. C. Early, J. Franklin Inst. 262, 17 (1956).
9. K. Bol, Phys. Fluids 7, 1855 (1964).
10. J. S. Serafini, Bull. Am. Phys. Soc. 13, 278 (1968).
11. J. S. Serafini, Bull. Am. Phys. Soc. 13, 1567 (1968).
12. J. S. Serafini, NASA TM X-1975 (1970).
13. K. Bol and R. A. Ellis, Bull. Am. Phys. Soc. 13, 263 (1968).
14. A. R. Akhmedov and A. A. Zaitsev, Soviet Phys.-Tech. Phys. 8, 126 (1963).
15. N. D'Angelo and L. Enriques, Phys. Fluids 9, 2290 (1966).
16. J. H. Noon, H. A. Schmidt and E. H. Holt, Plasma Phys. 12, 477 (1970).
17. J. R. Apel, Phys. Rev. Letters 19, 744 (1967).
18. J. R. Roth and W. M. Krawczonek, NASA TM X (to be published).

19. J. H. Malmberg, C. B. Wharton and W. E. Drummond, in Proceedings of the Second IAEA Conference on Plasma Physics and Controlled Nuclear Fusion Research (1965), Vol. 1, p. 485.

20. J. A. Schmidt, Rev. Sci. Instr. 39, 1297 (1968).

21. D. E. Lencioni, J. W. Poukey, J. A. Schmidt, J. C. Sprott and C. W. Erickson, Phys. Fluids 11, 1115 (1968).

22. J. R. Roth, D. C. Freeman, Jr., and D. A. Haid, Rev. Sci. Instr. 36, 1481 (1965).

23. J. R. Roth and M. Clark, Plasma Phys. 11, 131 (1969).

24. J. R. Roth, Rev. Sci. Instr. 37, 1100 (1966).

25. V. N. Tsytovich, "Stochastic Processes in Plasma," presented at the 9th International Conference on Phenomena in Ionized Gases, Bucharest, Romania (1969).

26. J. R. Roth, Phys. Fluids 10, 2712 (1967).

27. J. R. Roth, Phys. Fluids 12, 260 (1969).

28. S. M. Krivoruchko and E. A. Kornilov, Soviet Phys.-JETP Letters 10, 299 (1969).

E-6027

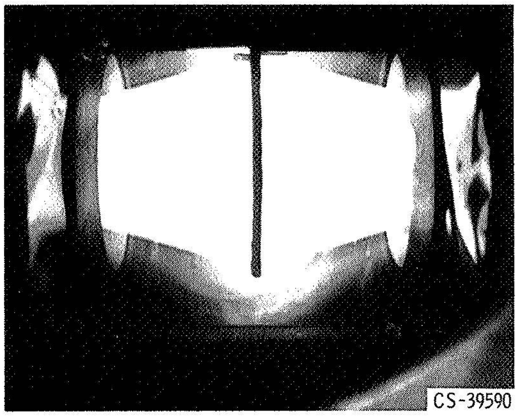

Figure 1

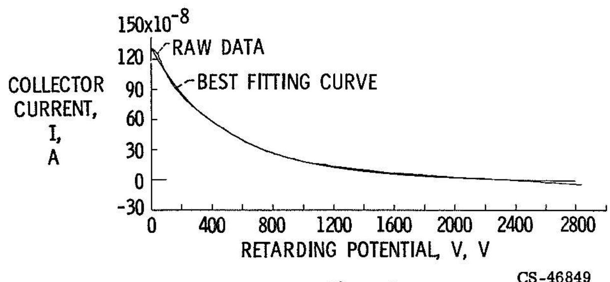

Figure 2

E-6027

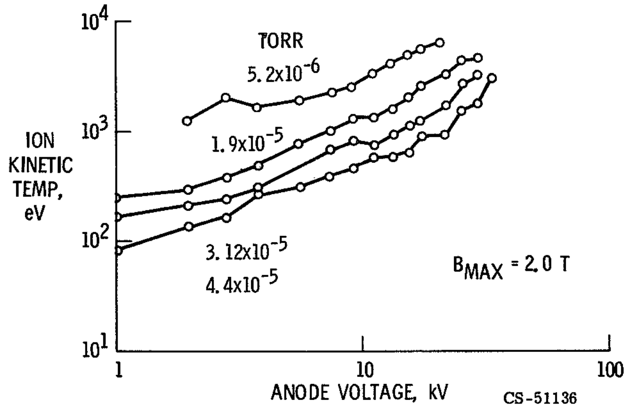

Figure 3

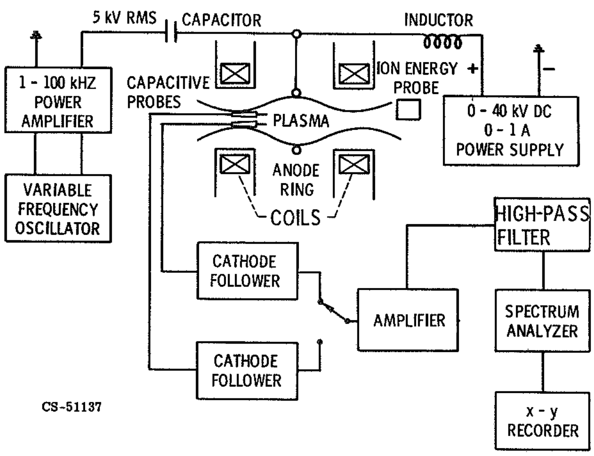

Figure 4

E-6027

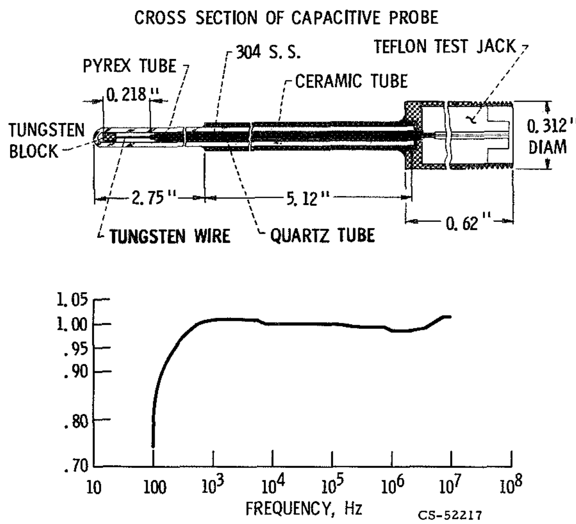

Figure 5

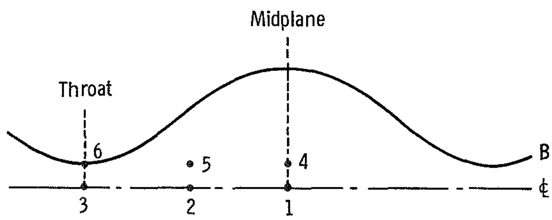

Figure 6

E-6027

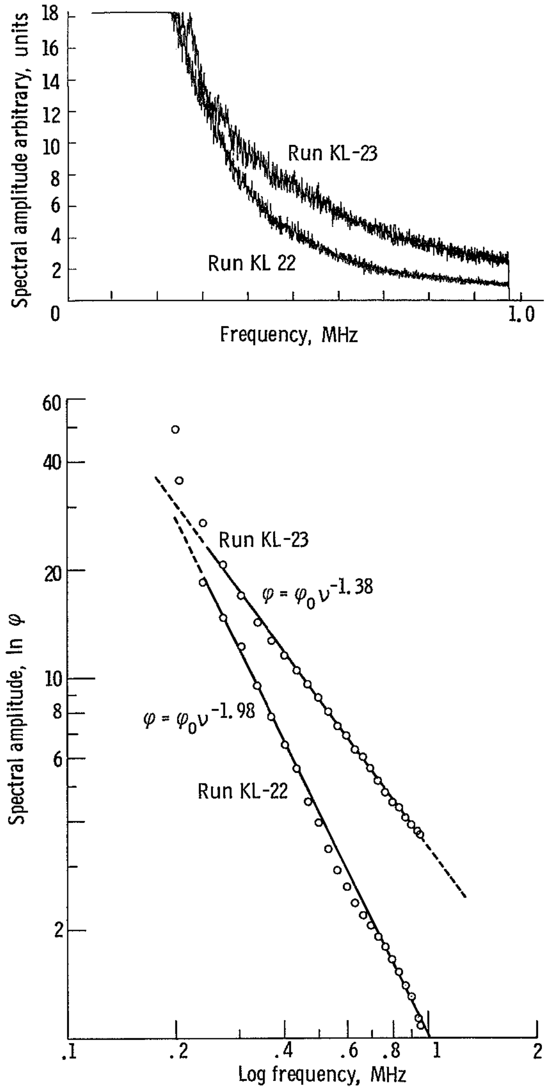

Figure 7

E-6027

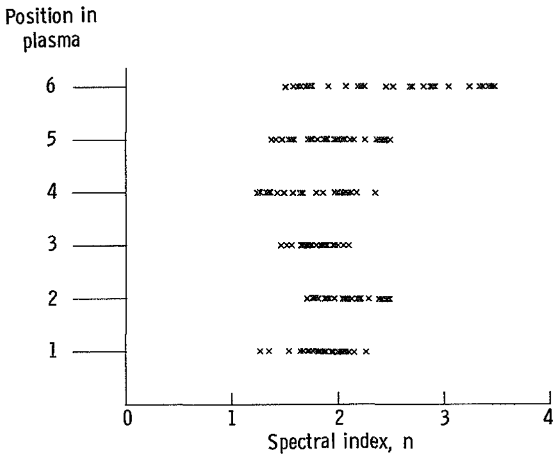

Figure 8. - Values of spectral index measured at various positions in plasma.

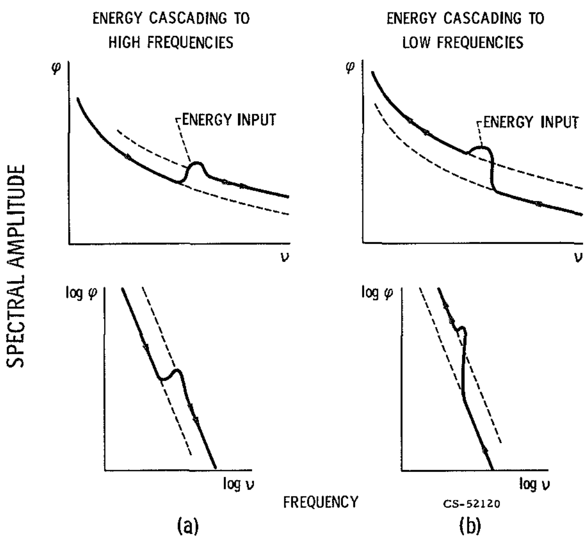

Figure 9

E-6027

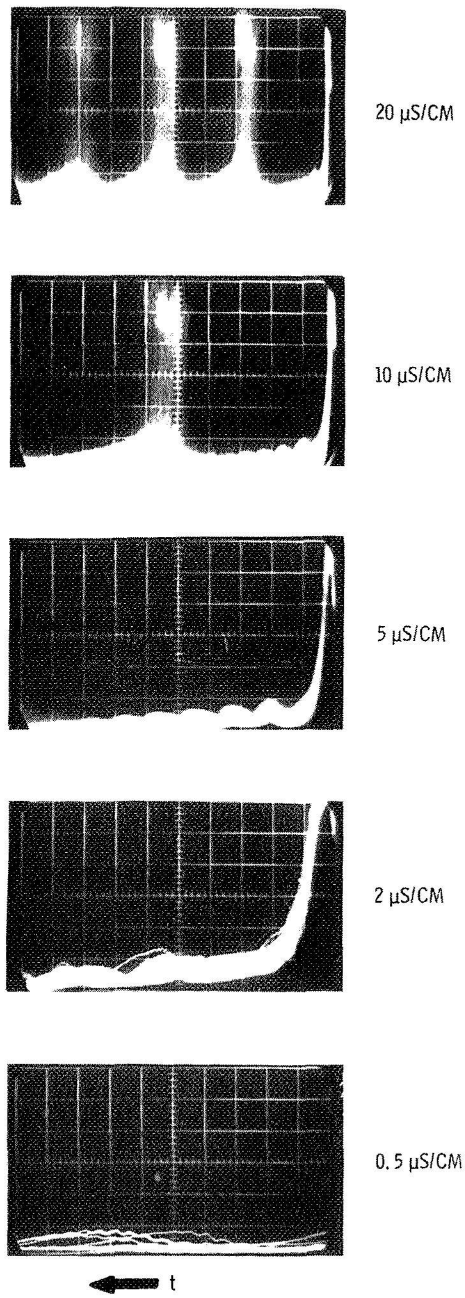

Figure 10

E-6027

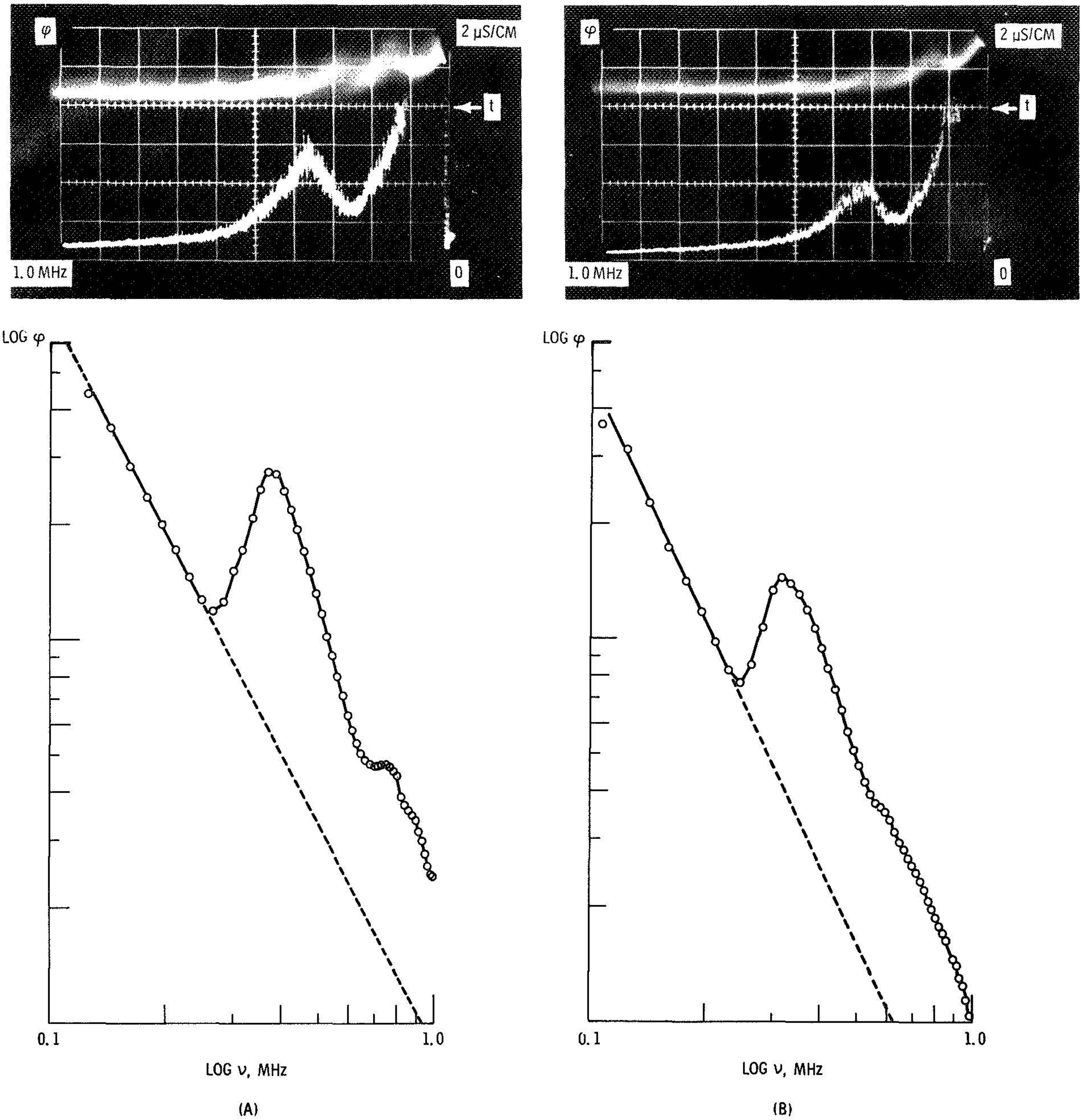

Figure 11

E-6027

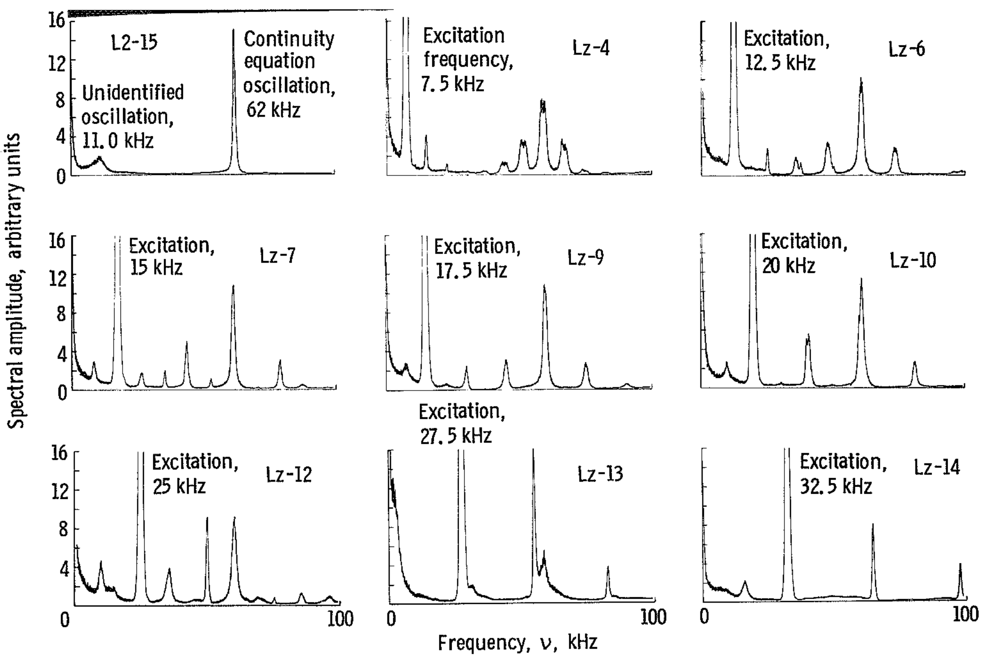

Figure 12

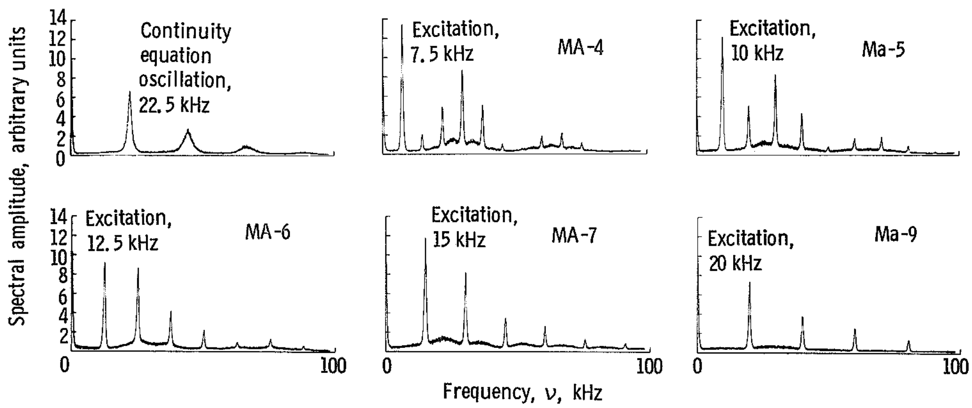

Figure 13

E-6027

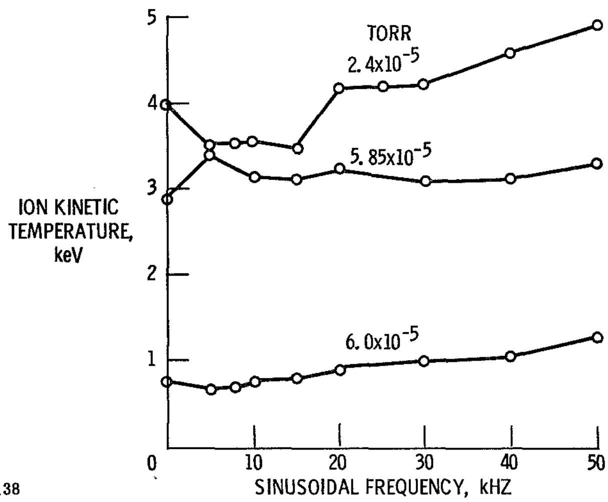

CS-51138

Figure 14